Optical microsphere resonators: optimal coupling to high-Q whispering-gallery modes

M. L. Gorodetsky and V. S. Ilchenko

Moscow State University, 119899, Moscow, Russia

Received May 27, 1997; revised manuscript received September 4, 1998

A general model is presented for coupling of high-Q whispering-gallery modes in optical microsphere resonators with coupler devices that possess a discrete and continuous spectrum of propagating modes. By contrast to conventional high-Q optical cavities, in microspheres the independence of high intrinsic quality-factor and controllable parameters of coupling via an evanescent field offer a variety of regimes similar to those that are already available in rf devices. The theory is applied to data reported earlier on different types of couplers to microsphere resonators and is complemented by the experimental demonstration of enhanced coupling efficiency (~80%) and variable loading regimes with $Q > 10^8$ fused-silica microspheres. © 1998 Optical Society of America [S0740-3224(98)01412-X]

OCIS codes: 270.0270, 290.4020, 250.5300, 060.1660.

1. INTRODUCTION

High-Q optical microsphere resonators currently are attracting growing interest in experimental cavity QED,[1–3] measurement science,[4,5] frequency stabilization, and other photonics applications.[6,7] Stemming from extensive studies of Mie resonances in microdroplets of aerosols[8] (observed by means of elastic and inelastic scattering of free-space beams), further studies of laboratory-fabricated solid-state microspheres are focusing on the properties and applications of highly confined whispering-gallery (WG) modes. Modes of this type possess negligible electrodynamically defined radiative losses (the corresponding radiative quality factors are $Q_{\mathrm{rad}} > 10^{20}$ and higher), are not accessible by free-space beams, and therefore require employment of near-field coupler devices. At present, in addition to the well-known prism coupler with frustrated total internal reflection[9,10] (TIR), coupler devices include side-polished fiber couplers[5,11,12] and fiber tapers.[13] The principle of all these devices is based on providing efficient energy transfer to the resonant circular TIR guided wave in the resonator (representing the WG mode) through the evanescent field of a guided wave or a TIR spot in the coupler.

It is evident *a priori* that efficient coupling can be expected on fulfillment of two main conditions, phase synchronism and significant overlap of the two waves that modeling the WG mode and the coupler mode. Although reasonable coupling efficiency has been demonstrated with three types of device (as much as a few tens of percent of input beam energy absorbed in a mode on resonance), no systematic theoretical approach has been developed to quantify the performance of coupler devices. It has still remained unclear whether it is possible at all and what the conditions are to provide complete exchange of energy between a propagating mode in a coupler device and the given WG mode in a high-Q microsphere. Answers to these questions are of critical importance for photonics applications and also for the proposed cavity QED experiments with microspheres.

In this paper we present a general approach to describe the near-field coupling of a high-Q WG mode with a propagating mode in a dielectric prism, slab, or waveguide structure. Theoretical results of this approach present a complete description of and give a recipe for obtaining optimal coupling with existing devices. We emphasize the importance of a loading quality factor parameter Q_c and its relation to the intrinsic Q_0 factor of WG modes as a crucial condition for obtaining optimal coupling. Our theoretical consideration is complemented by experimental tests of variable loading regimes and a demonstration of improved coupling efficiency with a prism coupler.

2. GENERAL CONSIDERATIONS

Let us examine excitation of a single high-Q WG mode with a high quality factor by (N) traveling modes in an evanescent wave coupler. This coupler can have either an infinite number of spatial modes ($N = \infty$, as in a prism coupler[9,10] and a slab) or only one mode ($N = 1$, as in a tapered fiber[13] and an integrated channel waveguide). We start with a simple description of the system, using lumped parameters and a quasi-geometrical approximation.

Let $A_0(t)$ be the amplitude of a circulating mode of TIR in the resonator (Fig. 1) to model the whispering-gallery mode. Let the pump power be distributed in the coupler between its modes such that $B_k(t)$ is the amplitude of mode k ($1 \leqslant k \leqslant N$) and $B^{\mathrm{in}}(t)$ is the slowly varying amplitude, with $\Sigma|B_k^{\mathrm{in}}(t)|^2 = |B^{\mathrm{in}}(t)|^2$ equal to the total pump power. Let us assume for simplicity that coupling between different modes is absent without the resonator.

Assuming that the coupling zone is much smaller than the diameter D of the resonator, we can introduce local

0740-3224/99/010147-08$15.00

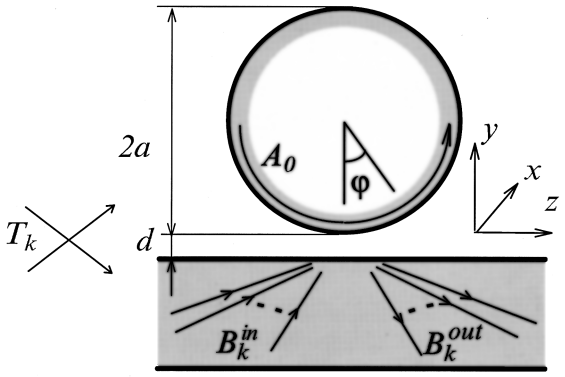

Fig. 1. Schematic of the excitation of WG modes in a high-Q microsphere.

real amplitude coefficients of transmittance T_k to describe the coupling of the resonator with all modes (either guided or leaky modes) of the coupler and the internal reflectivity coefficient R. We denote arrays of transmittance coefficients and amplitudes as vectors $\mathbf{T}$ and $\mathbf{B}$, respectively. If the quality factor of the resonator mode is high enough, a single circle will make only a small contribution to the mode buildup, and therefore $1 - R \ll 1$. In this case (neglecting for simplicity absorption and scattering losses in the coupler $R_k^2 = 1 - T_k^2$), we obtain

$$R = \prod R_k = 1 - \sum T_k^2/2 = 1 - T^2/2. \tag{1}$$

The equations for the mode of the resonator will be

$$\begin{aligned} A_0(t) &= i\sum T_k B_k^{\mathrm{in}}(t) + RA_0(t - \tau_0) \\ &\quad \times \exp(i2\pi n_s L/\lambda - \alpha L/2), \\ B_k^{\mathrm{out}}(t) &= R_k B_k^{\mathrm{in}}(t) + iT_k A_0(t), \end{aligned} \tag{2}$$

where $\tau_0 = n_s L/c$ is the circulation time for the mode traveling inside the sphere, $L \simeq 2\pi a$ is approximately equal to the circumference of the sphere, λ is the wavelength, n_s is the refractive index, c is the speed of light, and α is the linear attenuation in the resonator caused by scattering, absorption, and radiation.

In the above representation the microsphere is equivalent to a ring resonator formed by mirrors with transmittances T_k and filled with a lossy medium or, in case of single-mode coupling, as was pointed out in Ref. 11, to a Fabry–Perot resonator of length $L/2$ with a totally reflecting rear mirror.

If propagation losses are small, then near the resonance frequency $\omega_0 = 2\pi c/\lambda_0$ and $n_s L = m\lambda_0$, m an integer, by expanding $A_0(t - \tau_0) = A_0(t) - \tau_0 \mathrm{d}A_0/\mathrm{d}t$ from Eqs. (2) we obtain

$$\frac{\mathrm{d}A_0}{\mathrm{d}t} + (\delta_c + \delta_0 + i\Delta\omega)A_0 = iCB^{\mathrm{in}}, \tag{3}$$

where

$$\delta_0 = \frac{\alpha c}{2n_s}, \qquad \delta_c = \frac{1 - R}{R\tau_0} = \frac{T^2}{2\tau_0}, \qquad C = \frac{T\Gamma}{\tau_0}. \tag{4}$$

We introduce here another important coefficient,

$$\Gamma = \frac{\mathbf{TB}^{\mathrm{in}}}{TB^{\mathrm{in}}}. \tag{5}$$

This coefficient ($\Gamma \leqslant 1$) describes mode matching and shows how closely the field in the couplers matches the near field of resonator mode.

The term δ_0 originates from intrinsic quality factor $Q_0 = 2\pi n_s/\alpha\lambda$; δ_c describes loading, i.e., mode-energy escape to all modes of the coupler. Hereafter we mark all values associated with the coupler by the subscript c and values associated with the microsphere by the subscript s. Equation (3) is a classic equation for the amplitude of the resonator pumped by a harmonic field.

As is shown below, coefficients T_k can be calculated as normalized overlap integrals of the fields of the microsphere mode and modes of the coupler. The difference from a Fabry–Perot resonator is that, for the microsphere, coefficients T_k are not fixed parameters but instead depend strongly on the geometry of the coupling (e.g., exponentially on the value of the gap between the microsphere and the coupler) and are therefore in the hands of the experimentalist. As we have already emphasized,[9] it is the controllable relation between δ_0 and δ_c that defines the coupling efficiency in a given configuration (accounting both for mode overlap and synchronism and for optimized loading to provide an energy exchange between resonator and coupler). The stationary solution for Eq. (3) has the typical form

$$A_0 = \frac{i2\delta_c B^{\mathrm{in}}}{\delta_0 + \delta_c + i\Delta\omega}\frac{\Gamma}{T} = \frac{i\Gamma B^{\mathrm{in}}}{\delta_0 + \delta_c + i\Delta\omega}\left(\frac{2\delta_c}{\tau_0}\right)^{1/2}. \tag{6}$$

The field amplitude in the resonator will be maximum at $\delta_c = \delta_0$ (the intrinsic quality factor equals the loaded Q). The output stationary amplitudes are

$$\mathbf{B}^{\mathrm{out}} = \mathbf{B}^{\mathrm{in}} - B^{\mathrm{in}}\frac{2\delta_c\Gamma}{\delta_0 + \delta_c + i\Delta\omega}\frac{\mathbf{T}}{T}, \tag{7}$$

and the total output intensity in this case has a Lorentzian shape:

$$(B^{\mathrm{out}})^2 = (B^{\mathrm{in}})^2\left[1 - \frac{4\delta_c\delta_0\Gamma^2}{(\delta_0 + \delta_c)^2 + (\Delta\omega)^2}\right]. \tag{8}$$

It can easily be seen from Eq. (7) that the output signal can be considered the result of interference of the input and the reemission from the resonator. Note that the mode distribution of the second term in Eq. (7) (resonator mode emission pattern) does not depend on the input distribution.

The most important case of Eq. (7) is the regime of ideal matching ($\Gamma = 1$), obtained with $\mathbf{B}^{\mathrm{in}}/B^{\mathrm{in}} = \mathbf{T}/T$ when the fraction of the input power fed into the resonator mode is maximal. (A single-mode coupler is always mode matched.) In this case, provided that $\delta_c = \delta_0$, the output intensity becomes zero; i.e., the entire input power is lost inside the resonator. This regime is usually called critical coupling. Sometimes coupling is characterized by the fractional depth K of the resonance dip in intensity transmittance observed when the frequency of the exciting wave in the coupler is varied; from Eq. (8), K can be expressed as follows:

$$K = \frac{4Q_0Q_c\Gamma^2}{(Q_0 + Q_c)^2} = \frac{4Q\Gamma^2}{Q_0 + Q_c},$$
$$\frac{1}{Q} = \frac{2\delta_0}{\omega} + \frac{2\delta_c}{\omega} = \frac{1}{Q_0} + \frac{1}{Q_c}. \tag{9}$$

In the case of critical coupling, $K = 1$ (100%). In the case of nonideal matching, critical coupling can be observed until $2\Gamma^2 > 1$ (partial matching) if the output is mode filtered to pick up only part of the coupler modes. In this case leakage into other modes can be considered additional internal losses, and critical coupling is obtained with a lower loaded quality factor when $\delta_c = \delta_0/(2\Gamma^2 - 1)$. If $\delta_c \gg \delta_0$ (overcoupling), then for matched coupling the output wave in resonance has the sign opposite that out of resonance; i.e., the resonator shifts phase by π. It is appropriate to note here that, in traditional high-Q optical resonators that are composed of mirrors, the quality factor is limited by the mirrors' finesse, i.e., by loading. With microspheres the situation is opposite, and the primary role belongs to the intrinsic quality factor.

3. DIRECTIONAL COUPLER APPROACH

In this section it is our goal to determine the parameters of the coupler–resonator system from the electrodynamical point of view. A recent paper[14] by Rowland and Love (Love and Snyder are famous for their popular book on the theory of optical waveguides[15]) addressed the problem of coupling with WG modes on the basis of the model of distributed coupling between a traveling surface mode in a cylindrical resonator and a given mode in a planar (slab) waveguide. In this approach, the coupling problem leads to the necessity to solve a system of differential equations, which in our designations is as follows:

$$\frac{\mathrm{d}A_0}{\mathrm{d}z} = i\Delta\beta_0(z)A_0 + iC_k(z)\exp[i(\beta_k - \beta_0)z]B_k,$$
$$\frac{\mathrm{d}B_k}{\mathrm{d}z} = i\Delta\beta_k(z)B_k + iC_k(z)\exp[-i(\beta_k - \beta_0)z]A_0. \tag{10}$$

Coefficients $\Delta\beta_0(z)$ and $\Delta\beta_k(z)$ (which describe the perturbation of wave numbers β_0 and β_k of the modes of the resonator and the coupler) and distributed coupling coefficients c_k can be calculated explicitly as field cross-section integrals (see Ref. 14 and references therein):

$$\Delta\beta_0 = \frac{\omega(n_c^2 - 1)}{8\pi}\int_{\mathbf{C}}|\mathbf{e}_0|^2\mathrm{d}s,$$
$$\Delta\beta_k(z) = \frac{\omega(n_s^2 - 1)}{8\pi}\int_{\mathbf{S}}|\mathbf{e}_k|^2\mathrm{d}s,$$
$$C_k^2 = \frac{\omega^2}{64\pi^2}\int_{\mathbf{C}}(n_c^2 - 1)\mathbf{e}_k^*\mathbf{e}_0\mathrm{d}s\int_{\mathbf{S}}(n_s^2 - 1)\mathbf{e}_0^*\mathbf{e}_k\mathrm{d}s. \tag{11}$$

Here $\mathbf{e}_0$ and $\mathbf{e}_k$ are equivalent waveguide modes of the resonator and of the coupler, respectively, normalized versus power; the integration is done over the cross sections. Subscripts **S** and **C** denote that the integration is done inside the microsphere and the coupler, respectively. In principle, conservation of energy requires that the two integrals in the expression for C_k^2 be equal, and this is frequently postulated. However, in a common approximation that we also use here the above equality is operative only for phase-matched or identical waveguides, whereas in the opposite case the dependence of the two integrals on the gap is different. Nevertheless, for efficient coupling this equality must be satisfied.

Parameters (11) are nonzero only in the coupling zone. It may seem that the coupler transmission matrix and, subsequently, the lumped T_k coefficients introduced above can be found from Eqs. (10). However, an analytical derivation of the output field amplitudes cannot be found from Eqs. (10), except in a few simple cases. It was perhaps because of this fact that the authors of Ref. 14 presented only a numerical solution for their particular case. Moreover, in the general case the coupler transmission matrix is a complex 2×2 matrix and cannot be characterized by one real parameter.

Fortunately, the situation is more favorable for optical microsphere resonators with a high loaded quality factor $Q_c = \omega/2\delta_c$, when $T_k \ll 1$. Indeed, from Eqs. (4) it follows that $T^2 = m/Q$. In a fused-silica resonator with a diameter of 140 μm ($m \simeq 1000$) and heavily loaded $Q \simeq 10^7$ (the intrinsic Q factor can be of the order of 10^{10} in this case), $T \simeq 1\%$. In practice T is usually of the order of 10^{-3}, which means that field amplitude A_0 changes insignificantly over the coupling zone and can therefore be assumed to be constant in the second of Eqs. (10) and that the stationary amplitude $A_0 \gg B_k$. Therefore an approximate solution can be obtained:

$$A_0^{\mathrm{out}} = RA_0^{\mathrm{in}}\exp(i\Phi) + iT_kB_k^{\mathrm{in}},$$
$$B_k^{\mathrm{out}} = B_k^{\mathrm{in}} + iT_kA_0, \tag{12}$$

where

$$T_k = \int_{-\infty}^{\infty}C_k\exp[i(\beta_0 - \beta_k)z]\mathrm{d}z, \qquad \Phi = \int_{-\infty}^{\infty}\Delta\beta_0\mathrm{d}z. \tag{13}$$

Equations (12) are practically identical to Eqs. (2) if A_0 is closed into a ring. In the second of Eqs. (12) we neglected small second-order terms; however, we kept them in the first of Eqs. (12), as they describe the coupler-induced shift in resonant frequency and the reduction of Q by loading:

$$\omega_0 - \omega_0' = \frac{\Phi}{\tau_0} = \frac{\omega(n_c^2 - 1)}{8\pi\tau_0}\int_{\mathbf{C}}|\mathbf{e}_0|^2\mathrm{d}v,$$
$$\delta_c = \frac{T_k^2}{2\tau_0} = \frac{\omega^2(n_c^2 - 1)^2}{128\pi^2\tau_0}\left|\int_{\mathbf{C}}\mathbf{e}_k^*\mathbf{e}_0\exp[i(\beta_0 - \beta_k)z]\mathrm{d}v\right|^2. \tag{14}$$

4. VARIATIONAL APPROACH

The directional coupler approach can easily be generalized for a multimode coupler. However, expressions for the coupling parameters that are better suited for couplers with dense mode spectra can be found in a more rigorous way directly from Maxwell's equations by use of variational methods. The electric field in the resonator perturbed by the coupler can be written in the form

$$\mathbf{E}_s(\mathbf{r},\, t) \,=\, \exp(-i\omega t)\sum_j \hat{A}_j(t)\hat{\mathbf{e}}_j(\mathbf{r}), \tag{15}$$

where $\hat{\mathbf{e}}_j$ are orthonormalized eigenmodes of the unperturbed lossless resonator without the coupler:

$$\frac{1}{4\pi}\int \epsilon_s \hat{\mathbf{e}}_{j1}\hat{\mathbf{e}}^*_{j2}\mathrm{d}v \,=\, \delta_{j1,j2} \tag{16}$$

($\delta_{j1,j2}$ is the Kronecker symbol here). Rigorously speaking, this normalization encounters some difficulties for open dielectric resonators with the finite radiative quality factor Q_{rad}.[16] In the approach that we are considering, however, we can avoid them by assuming that the eigenfrequencies of interest ω_j are purely real. To do this we neglect the imaginary part that describes radiation losses and choose as the integration volume a sphere with a diameter much less than $Q_{\mathrm{rad}}\lambda/\pi$. Amplitudes $\hat{A}_j$ are slowly varying and differ from circulating amplitude A_j introduced above only in terms of normalization. One can easily see that

$$\frac{|\hat{\mathbf{e}}_j|^2}{|\mathbf{e}_j|^2} \,=\, \frac{c}{4\pi}\int_{\mathbf{S}}(\hat{\mathbf{e}}_j \times \hat{\mathbf{h}}^*_j)_z \mathrm{d}s \,=\, \frac{1}{\tau_j}. \tag{17}$$

The equation for the field in the coupled sphere will have the form

$$\nabla\times\nabla\times\mathbf{E}_s + \left[\frac{\epsilon_s(\mathbf{r})}{c^2} + \frac{\epsilon_c(\mathbf{r})\,-\,1}{c^2} + i\,\frac{2\delta_0\epsilon_s(\mathbf{r})}{\omega_0 c^2}\right]\frac{\partial^2\mathbf{E}_s}{\partial t^2} = -\frac{\epsilon_s(\mathbf{r})\,-\,1}{c^2}\,\frac{\partial^2\mathbf{E}_c}{\partial t^2}, \tag{18}$$

where the second term in brackets is additional polarization that is due to the presence of the coupler and the third term describes damping associated with intrinsic losses in the resonator; the right-hand side is the polarization caused by the pump wave. Dielectric susceptibilities $\epsilon_{s|c}(\mathbf{r})$ are equal to $n^2_{s|c}$ inside and to unity outside the spherical resonator and the coupler, respectively. Substituting Eq. (15) into Eq. (18) and multiplying the result by $\hat{\mathbf{e}}^*_0$, after integration over the entire volume and omitting small terms, we obtain

$$\frac{\mathrm{d}\hat{A}_0}{\mathrm{d}t} + \hat{A}_0(\delta_0 + i\Delta\omega') = \frac{i\omega(n_s^2\,-\,1)}{8\pi}\exp(i\omega t)\int_{\mathbf{S}}\mathbf{E}_c\hat{\mathbf{e}}^*_0\mathrm{d}v, \tag{19}$$

where $\Delta\omega' = \omega'_0 - \omega$ and

$$\omega'_0 \,=\, \omega_0 \,-\, \frac{\omega}{8\pi}\int_{\mathbf{C}}(n_c^2\,-\,1)|\hat{\mathbf{e}}_0|^2\mathrm{d}v \tag{20}$$

is the new resonance frequency shifted because of the coupler, in total agreement with Eqs. (14). Let us express the field in the coupler as an expansion in traveling modes in the z direction:

$$\mathbf{E}_c(\mathbf{r},\, t) \,=\, \exp(-i\omega t)\int B_\beta(z,\, t)\mathbf{e}_\beta(\mathbf{r})\exp(i\beta z)\mathrm{d}\beta. \tag{21}$$

Guided localized modes of the coupler in this description can also easily be taken into account if we choose B_β as

$$B_\beta \,=\, \sum_k B_k\delta(\beta\,-\,\beta_k) + \tilde{B}_\beta. \tag{22}$$

The coupler modes are normalized in such a way that

$$\frac{c}{4\pi}\int(\mathbf{e}_{\beta1}\times\mathbf{h}^*_{\beta2})_z\mathrm{d}s \,=\, \delta(\beta_1\,-\,\beta_2) \tag{23}$$

(here $\delta(\beta_1\,-\,\beta_2)$ is a delta function and $\mathbf{h}$ is the magnetic field corresponding to the mode). Integration is performed over the cross section that is orthogonal to the z axis. Amplitudes B_β (slowly varying with z and t) describe the distribution of the pump wave in coupler modes. Substituting Eq. (21) into the wave equation:

$$\nabla\times\nabla\times\mathbf{E}_c + \left[\frac{\epsilon_c(\mathbf{r})}{c^2} + \frac{\epsilon_s(\mathbf{r})\,-\,1}{c^2}\right]\frac{\partial^2\mathbf{E}_c}{\partial t^2} = -\frac{\epsilon_c(\mathbf{r})\,-\,1}{c^2}\,\frac{\partial^2\mathbf{E}_s}{\partial t^2}, \tag{24}$$

we obtain

$$\int\left[\beta\,\frac{\partial B_\beta}{\partial z} - \frac{i\omega^2(\epsilon_s\,-\,1)}{2c^2}\,B_\beta\right]\mathbf{e}_\beta\exp(i\beta z)\mathrm{d}\beta = \frac{i(\epsilon_c\,-\,1)\omega^2}{2c^2}\,\mathbf{E}_s\exp(i\omega t). \tag{25}$$

The second term in brackets in Eq. (24) determines the change of the wave number (phase velocity) for the given mode in the coupling zone. Taking the vector product of Eq. (25) with $\mathbf{h}^*_\beta$ and integrating over the cross section, we obtain formal solutions for slowly varying amplitudes:

$$B_\beta = B^{\mathrm{in}}_\beta\exp(i\Delta\beta z) + \frac{i\omega^2}{8\pi c\beta} \times\int_{-\infty}^{z}\exp[i\omega t\,-\,i\beta z' + i\Delta\beta(z\,-\,z')] \times\int_{\mathbf{C}}(n_c^2\,-\,1)(\mathbf{E}'_s\times\mathbf{h}'^*_\beta)_z\mathrm{d}s'\mathrm{d}z',$$

$$\Delta\beta(z) \,=\, \frac{\omega^2(n_s^2\,-\,1)}{8\pi c\beta}\int_{\mathbf{S}}(\mathbf{e}_\beta\times\mathbf{h}^*_\beta)_z\mathrm{d}s. \tag{26}$$

Substituting Eq. (21) into Eq. (19), using Eq. (26) and omitting $\Delta\beta$, we finally obtain the following equation for the amplitude of the mode in the resonator:

$$\frac{\mathrm{d}\hat{A}_0}{\mathrm{d}t} + (\delta_0 + \delta_c + i\Delta\omega')\hat{A}_0 = \frac{i\omega(n_c^2 - 1)}{8\pi} \int B_\beta^{\mathrm{in}} \int_{\mathbf{C}} \hat{\mathbf{e}}_0 \mathbf{e}_\beta^* \exp(-i\beta z)\mathrm{d}v\,\mathrm{d}\beta, \quad (27)$$

where

$$\begin{aligned}\delta_c &= \frac{\omega^3}{64\pi^2 c} \int\int_{\mathbf{S}} \int_{-\infty}^{-z} \int_{\mathbf{C}} \frac{(n_s^2 - 1)(n_c^2 - 1)}{\beta} \times \exp[i(\beta + \Delta\beta)(z - z')] \times (\hat{\mathbf{e}}_0' \times \mathbf{h}_\beta'^*)_z (\mathbf{e}_\beta \hat{\mathbf{e}}_0^*)\mathrm{d}s'\mathrm{d}z'\mathrm{d}v\mathrm{d}\beta \\ &\simeq \frac{\omega^2(n_c^2 - 1)^2}{128\pi^2} \int \left| \int_{\mathbf{C}} \hat{\mathbf{e}}_0 \mathbf{e}_\beta^* \exp(-i\beta z)\mathrm{d}v \right|^2 \mathrm{d}\beta, \end{aligned} \quad (28)$$

in natural agreement with Eqs. (14). Total agreement with Eqs. (3)–(7) becomes apparent if we put

$$T_\beta = \frac{\omega(n_c^2 - 1)}{8\pi} \int_{\mathbf{C}} \mathbf{e}_0 \mathbf{e}_\beta^* \exp[i(\beta_0 - \beta)z]\mathrm{d}v. \quad (29)$$

For high-Q WG modes $\beta_0 \simeq m/a$, and, as the field drops outside the resonator approximately as $\exp(-\gamma r)$ [$\gamma^2 \simeq k^2(n_s^2 - 1)$], the dependence of $\mathbf{e}_0$ on z can be approximated as follows: $\mathbf{e} \simeq \mathbf{e}(z = 0)\exp(-\gamma z^2/2a)$. If the coupler is straight in the z direction (as in most couplers demonstrated to date), we obtain

$$T_\beta = \frac{\omega(n_c^2 - 1)}{8\pi} \left(\frac{2\pi a}{\gamma}\right)^{1/2} \times \int_{\mathbf{C}} \exp[-(\beta a - m)^2/2\gamma a]\mathbf{e}_0 \mathbf{e}_\beta^* \mathrm{d}s. \quad (30)$$

5. APPLICATION TO DEMONSTRATED COUPLERS

Let us now use the approach that we have developed to analyze the coupling of WG modes with an optical fiber. As, according to Eq. (9), the possibility of efficient coupling depends critically on the value of the loading quality factor Q_c and its relation to the intrinsic Q, in this section we focus on the calculation of Q_c and discuss briefly methods to achieve phase synchronism and mode matching with different couplers.

To date, two types of optical fiber coupler to WG modes in microspheres have been demonstrated. The first type is the eroded fiber coupler,[5,11,12] in which the evanescent field of a propagating waveguide mode becomes accessible as a result of partial removal of the cladding in a bent section of the fiber. The recently demonstrated second type of fiber coupler is based on the stretched section of a single-mode fiber and employs the mode conversion of the initial guided wave into waveguide modes of cladding tapered to a diameter of few micrometers.

The most interesting types of strong confinement mode of the sphere, with radius a TE_{llq} (where radial index q is small) and the HE_{11} mode in the fiber of radius b, can be approximated as follows[15,17]:

$$\hat{\mathbf{e}}_s^x(r,\theta,\phi) \simeq \frac{2\sqrt{n_s^2 - 1}}{n_s^2 a^{3/2}} \left(\frac{l}{\pi}\right)^{1/4} \times \exp[-l(\pi/2 - \theta)^2/2 + il\phi] \times \begin{cases} j_l(kn_s r)/j_l(kn_s a) & r \leqslant a \\ \exp[-\gamma(r - a)] & r > a \end{cases}, \quad (31)$$

$$\mathbf{e}_c^x(\rho,\varphi) \simeq \frac{2\eta}{\gamma b\sqrt{n_c c}} \begin{cases} J_0(\eta\rho)/J_0(\eta b) & \rho \leqslant b \\ \exp[-\gamma(\rho - b)] & \rho > b \end{cases}, \quad (32)$$

where j_l and J_0 are, respectively, spherical and cylindrical Bessel functions and k is the wave number ($k = 2\pi/\lambda$). Here we give only the overlapping x components of the fields:

$$\begin{aligned}\eta b &\simeq 2.405 \exp\left(-\frac{1 + 1/n_c^2}{2b\gamma}\right) \simeq 2.405\left(1 - \frac{1 + 1/n_c^2}{2b\gamma}\right), \\ \gamma &\simeq [(l + 1/2)^2/a^2 - k^2]^{1/2} \simeq k\sqrt{n_s^2 - 1}. \end{aligned} \quad (33)$$

Using Eqs. (14) and (17) and expanding the Bessel functions in the coupling zone into Taylor series:

$$\begin{aligned} j_l(kn_s r) &\simeq j_l(kn_s a) + kn_s(r - a)j_l'(kn_s a) \\ &\simeq j_l(kn_s a) + kn_s(r - a)j_l'(t_{l+1/2,q}), \\ J_0(\eta\rho) &\simeq J_0(\eta b) + \eta(\rho - b)J_0'(\eta b) \\ &\simeq J_0(\eta b) + \eta(\rho - b)J_0'(t_{0,1}), \end{aligned} \quad (34)$$

where $t_{\nu,q}$ is the q zero of the Bessel function of order ν, we can now calculate

$$Q_c \simeq \frac{16\sqrt{2}\pi^5 n_s^4 n_c (n_s^2 - 1)^2}{9(n_c^2 - 1)} \frac{a^{3/2} b^3}{\lambda^{9/2}} \times \exp[2\gamma d + (l - \beta a)^2/\gamma a], \quad (35)$$

where d is the gap between the resonator and the fiber. In our calculations, when going to Cartesian coordinates we also considered that angles (ϕ, φ, and $\theta - \pi/2$) are small in the coupling zone.

To obtain optimal coupling one has to require matching the propagation constants in the argument of the second exponent of relation (35) ($l = \beta a$), as in Ref. 13. In this case, using approximations for the eigenfrequences in the resonator:

$$\begin{aligned} kn_s a &\simeq t_{l+1/2,q} - \frac{n_s}{\sqrt{n_s^2 - 1}} \\ &\simeq l + 1/2 + (l + 1/2)^{1/3}[3\pi(q - 1/4)]^{2/3}/2 - \frac{n_s}{\sqrt{n_s^2 - 1}}, \end{aligned} \quad (36)$$

and considering that $n_s \simeq n_c = n$, one can obtain the optimal radius of the fiber and the loaded Q:

$$b \simeq \frac{2.3a}{[(nka)^2 - l^2]^{1/2}} \simeq 0.51\left[\frac{a\lambda^2}{n^2(4q-1)}\right]^{1/3},$$

$$Q_c \simeq 102\left(\frac{a}{\lambda}\right)^{5/2} \frac{n^3(n^2-1)}{4q-1} \exp(2\gamma d). \quad (37)$$

Using relations (37), we can try to compare our calculations with the experimental data reported in Ref. 13 for $\lambda = 1.55\ \mu$m, $a = 85\ \mu$m, and $b = 1.7\ \mu$m. The measured Q was 2×10^6, with $K = 72\%$. Using Eq. (9), we obtain $Q_0 = 8.5 \times 10^6$ and $Q_c = 2.6 \times 10^6$. Calculations with relations (37) give $Q_c = 2.5 \times 10^6$, in agreement with the experiment.

It is appropriate to note here that, in principle, as follows from relation (35), the minimum of Q_c does not correspond to phase matching ($\beta = l/a$) and is shifted to smaller b. This minimum is also not very sharp ($\sim 2/\sqrt{l}$, several percent of β). However, this case deserves special consideration, because for smaller b the approximations that we use here will give a larger (more than 10%) error. It is also important that the loaded Q increases quickly with the size of the resonator (as $l^{5/2}$), and in this way the range of possible applications of such a coupler becomes restricted. Even for small fused-silica spheres, the optimal radius of the most common silica fiber does not correspond to single-mode operation, implying further technical complications in use of this type of coupler.

The conclusions of our theory also correlate with the data on limited efficiency of side-polished optical fiber couplers.[5,11,12] Indeed, with the typical monomode fibers that have core indices equal to or smaller than those of the spheres (made from polystyrene or silica),[5,11,12] with small microspheres one cannot satisfy phase matching because of the relatively large diameter of standard cores, and with larger spheres the coupling coefficient is too small (the coupling Q factor is too high) to provide efficient power insertion into the resonator.

Efficient coupling (tens of percent) with high-Q microspheres has been demonstrated with planar (slab) waveguides.[18] This type of coupler provides more freedom than fiber waveguides because it permits free manipulation of the two-dimensional optical beams. The optimal width of the two-dimensional beam (or width of the channel in the case of channel planar waveguides) for effective coupling has to be $g = \sqrt{2/l}a$. In the meantime, the requirement of phase matching for efficient coupling ($\beta = l/a$) implies optimization of the slab waveguide's effective thickness:

$$f \simeq \frac{\pi}{[n_c^2k^2 - \beta^2 - \gamma^2 - (\pi/g)^2]^{1/2}}. \quad (38)$$

Using the same approach as above, and assuming that the field distribution in the slab in the coupling zone is

$$\mathbf{e}_c^x(y) \simeq \frac{2\pi^{5/4}}{\gamma f^{3/2}\sqrt{ncg}} \exp(-x^2/2g^2) \times \begin{cases} \sin[\alpha(1/\gamma - y)]/\sin(\alpha/\gamma) & y \leqslant 0 \\ e^{-\gamma y} & y > 0, \end{cases}$$

$$\alpha^2 = n_c^2k^2 - \beta^2, \quad (39)$$

we obtain

$$Q_c \simeq \frac{8\pi^2 n_s^3 n_c(\sqrt{n_s^2-1} + n_s)(n_s^2-1)^{3/2}}{(n_c^2-1)^2} \frac{af^3}{\lambda^4} \times \exp[2\gamma d + (l - \beta a)^2/\gamma a]. \quad (40)$$

It is appropriate to note here that either fibers or planar waveguides can also effectively excite modes with $l \neq m$ if the wave vector is inclined to the equator plane of the sphere (symmetry plane of the residual ellipticity) by the angle $\arccos(m/l)$. This conclusion becomes evident if we remember that the mode with lmq is equivalent to a precessing inclined fundamental llq mode.[10]

A prism coupler was analyzed previously[9,10] together with the precession approach to the description of WG modes and theoretical and experimental investigation of the far-field patterns. By contrast to waveguide couplers, for which the practical realization of high efficiency implies either precise engineering of the waveguide parameters or the step-by-step search of the optimal contact point to the fiber taper, prism couplers permit a systematic procedure of coupling optimization by manipulating the external beams. The two steps to achieving efficient coupling are adjustment of the incidence angle Φ of the input Gaussian beam inside the coupler prism and adjustment of the angular size of the beam, $\Delta\Phi$ and $\Delta\Theta$, to provide mode matching with the far field of the WG mode in the prism (Γ factor):

$$\sin\Phi_0 = \frac{l}{n_c ka}, \qquad \Delta\Phi^2 = \frac{\sqrt{n_s^2-1}}{n_p^2 ka\cos^2\Phi_0},$$

$$\Delta\Theta^2 = \frac{n_s + \sqrt{n_s^2-1}}{n_p^2 ka}. \quad (41)$$

The loading Q with the prism coupler is

$$Q_c \simeq \frac{\sqrt{2}\pi^{5/2} n_s^{1/2}(n_s^2-1)}{(n_c^2-n_s^2)^{1/2}} \left(\frac{a}{\lambda}\right)^{3/2} \exp(2\gamma d). \quad (42)$$

Figure 2 summarizes the calculations of the loading quality factor for three types of coupler (with optimized

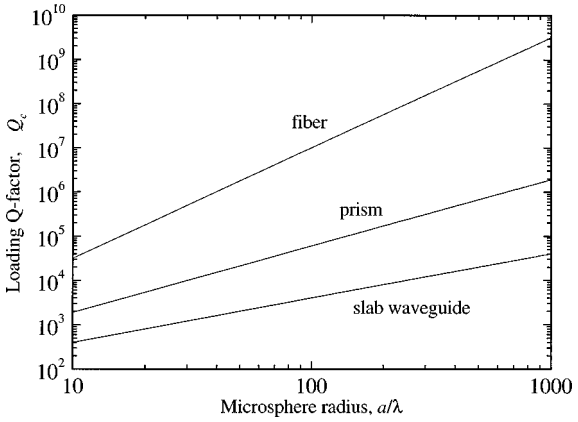

Fig. 2. Efficiency of three kinds of coupler in terms of the loading quality factor Q_c with optimized parameters at $d = 0$ as a function of sphere radius a; numerical results are obtained for the TM_{ll1} mode. Critical coupling is possible when the intrinsic quality factor of the WG mode, Q_0, is larger than Q_c [see Eq. (9)].

parameters) in the form of plots of Q_c under zero gap $d = 0$. The results shown in Fig. 2 allow us to evaluate quickly the possibility of achieving critical coupling with the given size and intrinsic Q of the sphere, along the lines summarized in Section 2 [Eq. (9)].

In our experiments employing high-Q WG microsphere resonators we used a prism coupler in most cases and believe that it remains the most flexible device, as it provides an ability for fine adjustment of both phase synchronism and mode matching by convenient manipulation of the apertures and the incidence angles of free beams. Also, as shown in Fig. 2, it provides a significant margin for obtaining critical coupling with spheres of various sizes and intrinsic values of Q. As a result, we routinely obtained coupling efficiencies to silica microspheres of ~30% with standard right-angle BK7 glass prisms, limited by restricted mode overlap caused by input refraction distortions of the symmetrical Gaussian beams. Use of cylindrical optics or higher-refraction prisms to eliminate the mode mismatch ($\Gamma \to 1$) can significantly improve coupling efficiency and approach a full exchange of energy under the critical regime. (Approximately 80% coupling efficiency is demonstrated in the Section 7 below.)

To conclude this section, let us also note here that the critical coupling (which is characterized by maximal absorption of the input power in the resonator) is in fact useless for such applications as cavity QED and quantum-nondemolition experiments, because no recirculated power escapes the cavity mode. To be able to utilize the recirculated light one has to provide the inequality $Q_c \ll Q_0$ (strong overcoupling). In other words, the intrinsic quality factor has to be high enough to provide reserve for sufficient loading by the optimal coupler.

6. PRISM COUPLER: EXPERIMENTAL EFFICIENCY AND VARIABLE LOADING REGIMES

To illustrate the results of our analysis we performed measurements to characterize coupling efficiency of the prism coupler with high-Q fused-silica microspheres. As in our previous experiments, we used microspheres fabricated of high-purity silica preforms by fusion in a hydrogen–oxygen microburner (see a description of the technique in Ref. 19). The focus of present experiment was on obtaining enhanced coupling by maximizing the mode matching:

$$\Gamma = \frac{\mathbf{TB}^{\mathrm{in}}}{TB^{\mathrm{in}}}, \tag{43}$$

along the lines briefly described in Section 2. In our experiment, to diminish astigmatic distortions of the input Gaussian beam at the entrance face of the coupler prism we used an equilateral prism of flint glass (SF-18; refractive index $n = 1.72$). As usual, the input beam (a symmetrical Gaussian beam from a single-mode piezotunable He–Ne laser) was focused onto the inner surface of the prism at the proximity point with the microsphere. The angle of incidence and the cross section of the input beam were then optimized to yield the maximum response of a chosen WG mode. Initial alignment was done on the basis of direct observation of resonance interference in the far field, with the frequency of the laser slowly swept across the resonance frequency of the mode. With the given choice of prism material, the optimal angle of incidence for excitation of WG modes, $q \simeq 1$ (close to the critical angle of total internal refraction at the silica–glass interface), was approximately 60 deg, so astigmatic distortions of the input beam at the entrance face of the prism were minimized.

After preliminary alignment, the coupling efficiency was further maximized on the basis of direct observation of the resonance absorption dip: Full intensity of the beam after the coupler prism was registered by a linear photodetector and monitored on a digital oscilloscope. Results obtained with a TM_{llq} mode (which possesses the strongest confinement of the field in the meridional direction) are presented in Fig. 3 in form of the resonance curves observed on successively decreasing coupling (stepwise increasing the gap). Figure 3 illustrates good agreement of theory with experiment: indeed, resonance transmission decreases with loading until the quality factor becomes a factor of 2 smaller than the intrinsic Q_0; after that, the intensity contrast of the resonance decreases. Figure 4 presents explicitly the plot of the fitted

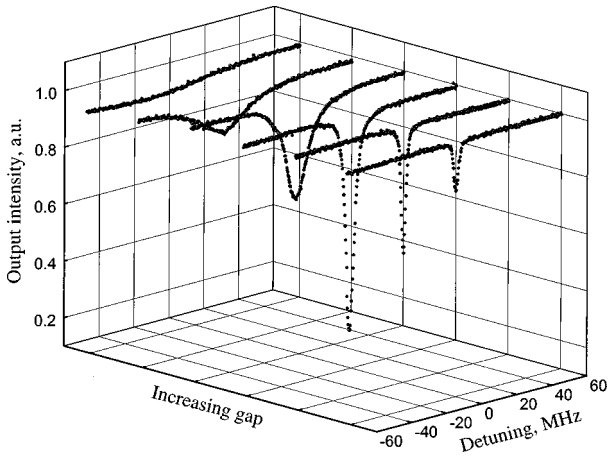

Fig. 3. Output intensity of the prism coupler observed under variable loading (successively increasing microsphere-prism gap). Fused-silica sphere with 270-μm diameter.

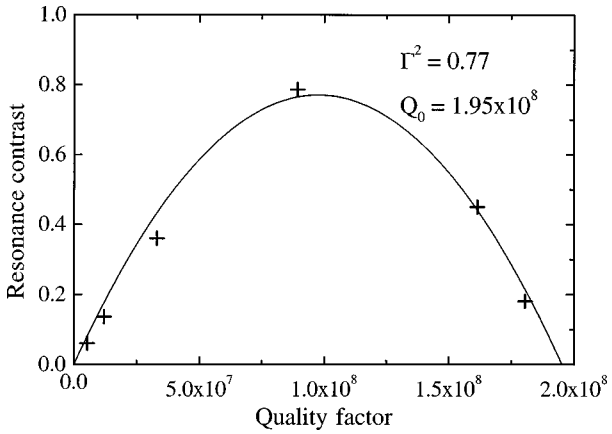

Fig. 4. Resonance contrast as a function of the loaded quality factor.

experimental intensity dip versus the loaded quality factor $Q = Q_c Q_0/(Q_c + Q_0)$, which yields satisfactory agreement with the parabolic prediction from the generalized expression [Eq. (9)]. The maximum contrast of the resonance obtained in our experiment was $K^2 \simeq 0.79$ (the deepest curve in Fig. 3).

7. CONCLUSION

We have presented a general approach to describing the near-field coupling of high-Q whispering-gallery modes in optical microsphere resonators to guided or free-space traveling waves in coupler devices with continuous and discrete spectra of propagating modes.

A convenient formalism of the loaded quality factor to describe the energy exchange between coupler modes and the resonator provides a quick algorithm for determining the efficiency of a given type of the coupler under a given value of the intrinsic quality factor of WG modes.

A variable relation between the intrinsic Q factor and the loading losses (described by Q_c) through energy escape to coupler modes is a distinctive new property of WG resonators compared with conventional Fabry–Perot cavities: The latter are characterized by fixed coupling through the reflectivities of the low-loss mirrors of which they are composed. This unique ability to control the Q and the coupling by means of the WG mode evanescent field allows us to obtain new regimes in the devices that are analogous to those available in lumped-element rf and microwave engineering.

Theoretical estimates on the basis of the suggested theory are in good agreement with the reported data on the efficiency of different coupler devices, including tapered, side-polished fiber, and slab waveguides.

Original experimental results include a direct demonstration of variable loading and enhanced efficiency (as much as ~80%) in a prism coupler. Ease of control of phase synchronism and mode overlap between the coupler and the microsphere mode by adjustment of the input beam parameters make the prism coupler versatile and efficient for various applications of high-Q microsphere resonators.

In conclusion, let us note that near-field coupling may be not a unique method for efficiently exciting highly confined WG modes in microspheres. Simple estimates show that, for example, recent advances in optical fiber grating fabrication methods[20] may permit a Bragg-type critical coupler for high-Q WG modes to be imprinted directly upon a sphere made from low-loss germanosilicate glass. This configuration might be of special interest for atomic cavity QED experiments, for which the presence of bulky external couplers may destroy the field symmetry, complicate laser cooling of atoms, etc.

ACKNOWLEDGMENT

This research was supported in part by Russian Foundation for Fundamental Research grant 96-15-96780.

REFERENCES

1. V. B. Braginsky, M. L. Gorodetsky, and V. S. Ilchenko, "Quality-factor and nonlinear properties of optical whispering-gallery modes," Phys. Lett. A **137**, 393–396 (1989).
2. H. Mabuchi and H. J. Kimble, "Atom galleries for whispering atoms: binding atoms in stable orbits around a dielectric cavity," Opt. Lett. **19**, 749–751 (1994).
3. V. Sandoghdar, F. Treussart, J. Hare, V. Lefèvre-Seguin, J.-M. Raimond, and S. Haroche, "A very low threshold whispering gallery mode microsphere laser," Phys. Rev. B **54**, R1777–R1780 (1996).
4. S. Schiller and R. L. Byer, "High-resolution spectroscopy of whispering gallery modes in large dielectric spheres," Opt. Lett. **16**, 1138–1140 (1991).
5. A. Serpengüzel, S. Arnold, and G. Griffel, "Excitation of resonances of microspheres on an optical fiber," Opt. Lett. **20**, 654–656 (1994).
6. V. V. Vasiliev, V. L. Velichansky, M. L. Gorodetsky, V. S. Ilchenko, L. Hollberg, and A. V. Yarovitsky, "High-coherence diode laser with optical feedback via a microcavity with 'whispering gallery' modes," Quantum Electron. **26**, 657–658 (1996).
7. L. Collot, V. Lefèvre-Seguin, M. Brune, J.-M. Raimond, and S. Haroche, "Very high-Q whispering gallery modes resonances observed on fused silica microspheres," Europhys. Lett. **23**, 327–333 (1993).
8. P. W. Barber and R. K. Chang, *Optical Effects Associated with Small Particles* (World Scientific, Singapore, 1988).
9. S. P. Vyatchanin, M. L. Gorodetsky, and V. S. Ilchenko, "Tunable narrowband optical filters with whispering gallery modes," Zh. Prikl. Spektrosk. **56**, 274–280, 1992.
10. M. L. Gorodetsky and V. S. Ilchenko, "High-Q optical whispering gallery microresonators: precession approach for spherical mode analysis and emission patterns," Opt. Commun. **113**, 133–143 (1994).
11. G. Griffel, S. Arnold, D. Taskent, A. Serpengüzel, J. Connoly, and N. Morris, "Morphology-dependent resonances of a microsphere-optical fiber system," Opt. Lett. **21**, 695–697 (1995).
12. N. Dubreuil, J. C. Knight, D. Leventhal, V. Sandoghdar, J. Hare, V. Lefévre-Seguin, J. M. Raimond, and S. Haroche, "Eroded monomode optical fiber for whispering-gallery mode excitation in fused-silica microspheres," Opt. Lett. **20**, 1515–1517 (1995).
13. J. C. Knight, G. Cheung, F. Jacques, and T. A. Birks, "Phase-matched excitation of whispering gallery mode resonances using a fiber taper," Opt. Lett. **22**, 1129–1131 (1997).
14. D. R. Rowland and J. D. Love, "Evanescent wave coupling of whispering gallery modes of a dielectric cylinder," Proc. Inst. Electr. Eng. Part J. **140**, 177–188 (1993).
15. A. W. Snyder and J. D. Love, *Optical Waveguide Theory* (Chapman & Hall, London, 1983).
16. H. M. Lai, P. T. Leung, K. Young, P. W. Barber, and S. C. Hill, "Time-independent perturbation for leaking electromagnetic modes in open systems with application to resonances in microdroplets," Phys. Rev. A **41**, 5187–5198 (1990).
17. S. Shiller, "Asymptotic expansion of morphological resonance frequencies in Mie scattering," Appl. Opt. **32**, 2181–2185 (1993).
18. N. Dubreuil, Institut d'Optique, Centre Universitaire d'Orsay, B.P. 147, 91403 Orsay cedex, France (personal communication, 1997).
19. M. L. Gorodetsky and V. S. Ilchenko, "Thermal nonlinear effects in optical whispering-gallery microresonators," Laser Phys. **2**, 1004–1009 (1992).
20. D. S. Starodubov, V. Grubsky, J. Feinberg, B. Kobrin, and S. Juma, "Bragg grating fabrication in germanosilicate fibers by use of near-UV light: a new pathway for refractive index changes," Opt. Lett. **22**, 1086–1088 (1997).